Comparison of electrical characteristic between AlN/GaN and AlGaN/GaN heterostructure Schottky diodes*

Lü Yuan-Jie(吕元杰)[a], Feng Zhi-Hong(冯志红)[a]†, Lin Zhao-Jun(林兆军)[b], Gu Guo-Dong(顾国栋)[a], Dun Shao-Bo(敦少博)[a], Yin Jia-Yun(尹甲运)[a], Han Ting-Ting(韩婷婷)[a], and Cai Shu-Jun(蔡树军)[a]

[a] *Science and Technology on Application-Specific Integrated Circuit Laboratory, Hebei Semiconductor Research Institute, Shijiazhuang* 050051, *China*
[b] *School of Physics, Shandong University, Jinan* 250100, *China*

(Received 20 March 2013; revised manuscript received 28 April 2013; published online 10 December 2013)

Ni/Au Schottky contacts on AlN/GaN and AlGaN/GaN heterostructures are fabricated. Based on the measured current–voltage and capacitance–voltage curves, the electrical characteristics of AlN/GaN Schottky diode, such as Schottky barrier height, turn-on voltage, reverse breakdown voltage, ideal factor, and the current-transport mechanism, are analyzed and then compared with those of an AlGaN/GaN diode by self-consistently solving Schrödinger's and Poisson's equations. It is found that the dislocation-governed tunneling is dominant for both AlN/GaN and AlGaN/GaN Schottky diodes. However, more dislocation defects and a thinner barrier layer for AlN/GaN heterostructure results in a larger tunneling probability, and causes a larger leakage current and lower reverse breakdown voltage, even though the Schottky barrier height of AlN/GaN Schottky diode is calculated to be higher that of an AlGaN/GaN diode.

Keywords: Al(Ga)N/GaN, Schottky barrier height, current-transport mechanism, leakage current

PACS: 71.55.Eq, 73.30.+y, 85.30.Mn, 11.40.–q **DOI:** 10.1088/1674-1056/23/2/027101

1. Introduction

For many years, AlGaN/GaN heterostructure field-effect transistors (HFETs) have been the subject of intense investigation due to their importance for microwave and high temperature/high power applications.[1–3] Nowadays, up-to-date materials of AlN/GaN heterostructure are of great advantage for high frequency operation, since AlN offers the greatest potential as a scalable barrier material among $Al_xGa_{1-x}N$ alloy compositions due to its large bandgap and polarization effects.[4,5] The best frequency (f_{max}/f_T: 342 GHz/518 GHz) is obtained on the AlN/GaN heterostructure due to the thin barrier layer and polarization effects.[6] However, little attention has been paid to the electrical characteristics of AlN/GaN heterostructure Schottky diodes, such as Schottky barrier height (φ_B), turn-on voltage (V_{on}), ideal factor (n), reverse breakdown voltage (V_b), and the current-transport mechanism, even though these characteristics are of great importance for device performance and reliability. The low breakdown voltage seriously hinders the application of AlN/GaN HFET in a high-power field, which is attributed to the large leakage current. Investigation of the electrical characteristic relation to the current transport is essential to improve the breakdown voltage of an AlN/GaN device. Since AlN/GaN and AlGaN/GaN heterostructures are both main-stream materials for microwave devices and digital circuits, comparing the electrical characteristics of an AlN/GaN diode with those of AlGaN/GaN diodes is of great importance to further improve the performance of GaN-based frequency devices and digital circuits.

In this paper, Ni/Au Schottky contacts on AlN/GaN and AlGaN/GaN heterostructures are prepared. From the measured current–voltage (I–V) curves and the capacitance–voltage (C–V) curves, the Schottky barrier height, the turn-on voltage, the ideal factor, and the reverse breakdown voltage of each sample are obtained and compared by self-consistently solving Schrödinger's and Poisson's equations. Furthermore, the models of thermionic-emission, generation–recombination, tunneling, surface leakage currents are all taken into account to investigate the current-transport mechanisms for AlN/GaN and AlGaN/GaN diodes. Based on the obtained Schottky barrier height and current-transport mechanism, the defects existing in the barrier layer are calculated and compared within AlN/GaN and AlGaN/GaN diodes.

2. Experiment

The AlN/GaN and AlGaN/GaN heterostuctures employed in this work are both epitaxially grown by metal organic chemical vapor deposition (MOCVD) on (0001) sapphire substrates. The AlN/GaN heterostructure is formed of a low-temperature nucleation layer followed by a 2-μm S. I. GaN, a 3-nm AlN barrier layer, and a 1-nm S. I. GaN cap. Hall measurements indicate a sheet carrier density of around 1.05×10^{13} cm^{-2} and an electron mobility of 1650 cm^2/V·s at room temperature. The AlGaN/GaN heterostructure is of a low-temperature nucleation layer followed by a 2-μm S. I. GaN, a 1-nm AlN interlayer, and finally a 22.5-nm thick undoped $Al_{0.3}Ga_{0.7}N$ barrier layer. Hall measurements indi-

*Project supported by the National Natural Science Foundation of China (Grant Nos. 60890192, 60876009, and 11174182).
†Corresponding author. E-mail: blueledviet@yahoo.com.cn
© 2014 Chinese Physical Society and IOP Publishing Ltd

cate a sheet carrier density of around 1.07×10^{13} cm^{-2} and an electron mobility of 1800 cm^2/V·s at room temperature. Uniform device processing is performed on the two different heterostructures. Ohmic contacts of Ti/Al/Ni/Au are fabricated by e-beam evaporation and lift-off. The Ohmic contacts are of a ring shape with an inner diameter of 600 μm and an outer diameter of 650 μm. A rapid thermal annealing is taken to form good Ohmic contacts. With transmission line method patterns, the specific resistivities of the Ohmic contacts are measured to be 5.1×10^{-5} Ω·cm^2 and 5.9×10^{-5} Ω·cm^2, respectively. Ni/Au (50 nm/200 nm) circular Schottky contacts with a diameter of 300 μm are finally deposited by e-beam evaporation. *C*–*V* measurements are performed at room temperature using an Agilent B1520A at 100 kHz, and the *I*–*V* characteristics are measured at room temperature using Keithley 4200 semiconductor parameter analyzer.

3. Calculation and analyses

Figure 1 shows the measured *C*–*V* curves under 100 kHz for AlN/GaN and AlGaN/GaN Schottky diodes, respectively. The two-dimensional electron gas (2DEG) electron density n_{2D} under zero gate bias can be obtained by integrating the measured *C*–*V* curve[7]

$$n_{2D} = \int_{V_T}^{0} \frac{C\,\mathrm{d}V}{(Sq)}, \tag{1}$$

where C is the measured capacitance between the Ohmic contact and the Ni Schottky contact, V_T is the threshold voltage and can be obtained by integrating the *C*–*V* curve (as shown in Fig. 1),[7] and S is the Ni Schottky contact area. The calculated 2DEG electron densities for AlN/GaN and AlGaN/GaN Schottky diodes are summarized in Table 1.

Figure 2 shows the measured *I*–*V* curves for AlN/GaN and AlGaN/GaN Schottky diodes, respectively. According to Chen *et al.*'s two-diode model,[8] an Al(Ga)N/GaN structure consisting of a metal gate can be considered as two diodes connected in series back to back. The first diode (diode 1) represents the Schottky contact between the Schottky metals and the Al(Ga)N barrier layer, the second diode (diode 2) represents the effective Schottky contact between the Al(Ga)N barrier layer and the 2DEG.[8,9] As shown in Fig. 2, the forward bias of structure current is an exponential function of the applied-bias voltage in the intermediate voltage regime (0.1 V$\leq V \leq$ 0.6 V for AlN/GaN diode, 0.9 V$\leq V \leq$ 1.4 V for AlGaN/GaN diode). It is clear that over a broad range (10^{-6}–10^{-3} A) of the forward current, the behavior is exponential and beyond that ($I > 10^{-3}$ A) the plots deviate from this behavior due to the effect of diode 2 and series resistance (R_S).[8–10] Based on the calculated 2DEG density, the Schottky barrier heights and ideal factor (n) values of the AlN/GaN and AlGaN/GaN Schottky diodes can be calculated from the *I*–*V* curves by self-consistently solving Schrödinger's and Poisson's equations.[9] The calculated results are shown in Table 1. The Schottky barrier height of the AlN/GaN Schottky diode is calculated to be higher than that of the AlGaN/GaN diode due to the larger bandgap of AlN.

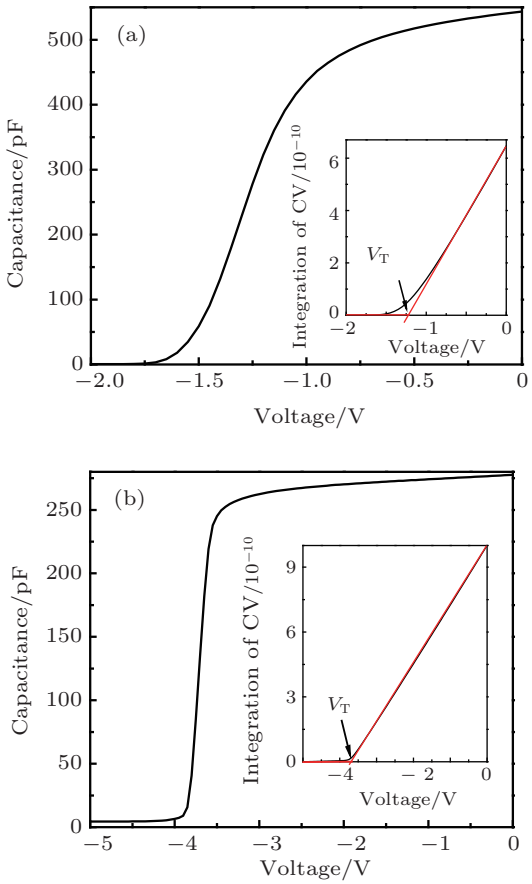


Fig. 1. (color online) Measured *C*–*V* curves under 100 kHz for the prepared AlN/GaN (a) and AlGaN/GaN (b) Schottky diodes.

Table 1. Calculated electrical characteristic parameters of AlN/GaN and AlGaN/GaN Schottky diodes.

	$n_{2D}/10^{12}$ cm^{-2}	φ_B/eV	V_{on}/V	V_b/V	n
AlN/GaN	5.72	2.08	0.93	180	2.16
AlGaN/GaN	8.86	1.60	1.32	240	1.57

As shown in Fig. 2 the values of turn-on voltage (V_{on}) are determined to be 0.93 V and 1.32 V for AlN/GaN and AlGaN/GaN Schottky diodes, respectively. A lower turn-on voltage indicates that the AlN/GaN Schottky diode has lower power dissipation while it almost maintains the same forward saturation current with AlGaN/GaN Schottky diode (shown in Fig. 2).

Figure 3 shows the measured reverse breakdown characteristics for AlN/GaN and AlGaN/GaN Schottky diodes, respectively. The reverse breakdown voltages are measured to be 180 V and 240 V for AlN/GaN and AlGaN/GaN Schottky diodes, respectively (shown in Fig. 3). In general, a larger

barrier height induces lower reverse leakage current and larger reverse breakdown voltage.[11] However, the AlN/GaN Schottky diode suffers larger leakage current and smaller breakdown voltage than the AlGaN/GaN Schottky diode (shown in Figs. 2 and 3). To explain the above phenomenon, the current-transport mechanism and the defects existing in the barrier layer for AlN/GaN and AlGaN/GaN diodes are investigated and compared.

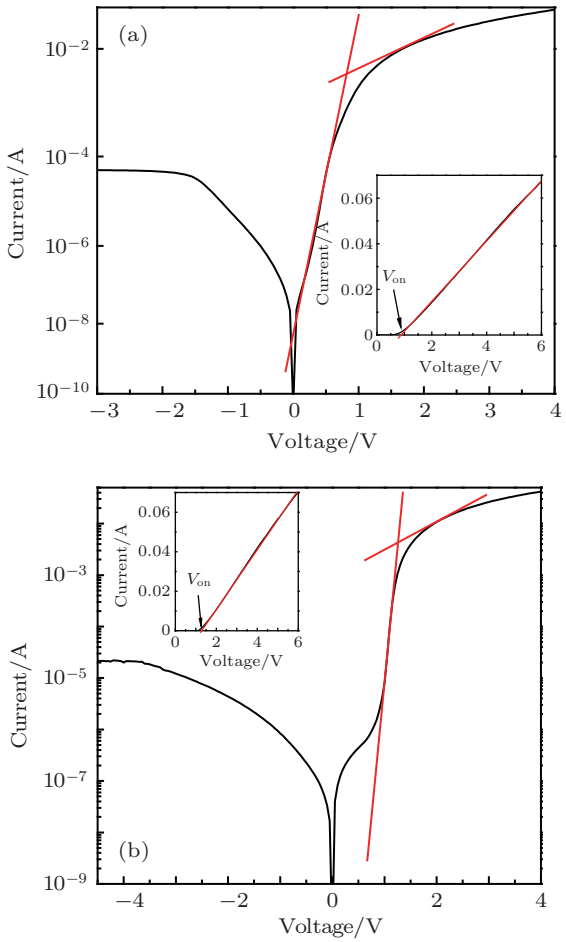


Fig. 2. (color online) Measured I–V curves of the prepared AlN/GaN (a) and AlGaN/GaN (b) Schottky diodes.

The forward current for the Al(Ga)N/GaN Schottky diode mainly consists of thermionic emission (TE) current ($I_{\text{thermionic}}$), generation–recombination current (I_{gr}), tunneling current (I_{tunnel}), and surface leakage current (I_{sur}) caused by the inhomogenities and defects at the M/S interface.[12] The total current of device can be expressed as

$$I_{\text{total}} = I_{\text{thermionic}} + I_{\text{gr}} + I_{\text{tunnel}} + I_{\text{sur}}. \tag{2}$$

In general, the relationship between the applied-bias voltage and the current of the Schottky diodes, based on the TE theory, is given by[13]

$$I_{\text{thermionic}} = I_0 \left\{ \exp\left[\frac{q(V - IR_{\text{S}})}{kT} \right] - 1 \right\}, \tag{3}$$

where I_0 is the saturation current, T is the absolute temperature, k is Boltzmann's constant, and q is the electron charge.

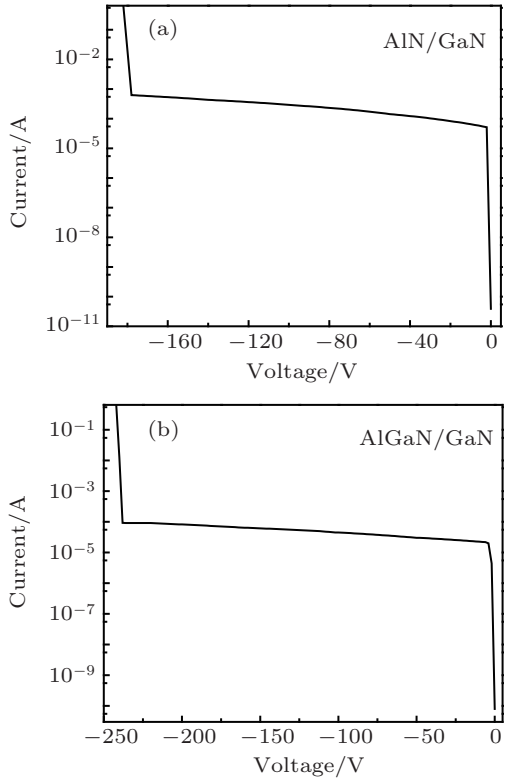


Fig. 3. Measured reverse breakdown characteristics of the prepared AlN/GaN (a) and AlGaN/GaN (b) Schottky diodes.

The generation–recombination current (I_{gr}) can be described by the relation[14]

$$I_{\text{g-r}} = I_{\text{gr}} \left\{ \exp\left[\left[\frac{q(V - IR_{\text{S}})}{2kT} \right] - 1 \right\}, \tag{4}$$

where I_{gr} is the generation–recombination saturation current. The tunneling current (I_{tunnel}) through the barrier is given by[13,15]

$$I_{\text{tunnel}} = I_{\text{t}} \left\{ \exp\left[\frac{q(V - IR_{\text{S}})}{E_0} \right] - 1 \right\}, \tag{5}$$

where I_{t} is the tunneling saturation current, and E_0 is the tunneling parameter defined as[15]

$$E_0 = E_{00} \coth\left(\frac{E_{00}}{kT} \right), \tag{6}$$

with E_{00} being the characteristic tunneling energy that is related to the tunnel effect transmission probability. In addition, voltage-proportional leakage current (I_{sur}) frequently changes the current–voltage (I–V) relationship at lower bias voltage levels and can be expressed as[15,16]

$$I_{\text{sur}} = \frac{V - IR_{\text{S}}}{R_{\text{sh}}}. \tag{7}$$

In order to determine the true current-transport mechanisms for AlN/GaN and AlGaN/GaN Schottky diodes, by taking the I_0, I_{gr}, I_{t}, the tunneling parameter E_0 and R_{sh} as adjustable fit parameters, we fit the experimental I–V data to the

analytical expressions given for the current-transport mechanisms in a wide range of applied biases.[12] The series resistance R_S can be obtained by plotting the $d(V)/d(\ln I)$ versus I.[17] As shown in Fig. 4, the voltage-proportional leakage current (I_{sur}) dominates the forward current at lower bias voltage for each of AlN/GaN and AlGaN/GaN Schottky diodes. There is excellent agreement between the data from the measured I–V curve and those from the current-transport expression for the tunneling mechanism in the intermediate voltage regime. However, there are no good fittings between the data from the measured I–V and the data from the analytic expression given for TE, generation–recombination, or the leakage current mechanism (Fig. 4). The values of the tunneling parameter E_0 and characteristic tunneling energy E_{00}, as determined from the fittings of the tunneling current expression to the measured I–V data set, are summarized in Table 2. A larger value of tunneling energy E_{00} of AlN/GaN diode indicates a bigger tunneling probability through the barrier.[15] According to the dislocation model of the tunneling current, the tunneling saturation current (I_t) can be described by the following equation[12]

$$I_t = qD\upsilon_D \exp(-qV_K/E_0). \tag{8}$$

where D is the dislocation density (DD), υ_D the Debye frequency, and V_K the diffusion potential for the Schottky barrier diode. By using $\upsilon_D = 1.68\times10^{13}$ s^{-1}, $V_K = 1.15$ eV for both AlN/GaN and AlGaN/GaN diodes and the determined $I_t(0)$ and E_0 from the measured I–V characteristic, the DDs of AlN/GaN and AlGaN/GaN diodes are obtained and summarized in Table 2. The details of the calculation can refer to Ref. [12]. Due to the larger Schottky barrier height, the value of V_K of AlN/GaN diode is larger than that of the AlGaN/GaN diode. However, even using the same value of V_K the calculated DD of AlN/GaN diode is much larger than that of the AlGaN/GaN diode (Table 2). The larger DDs in the AlN/GaN diode may be due to the larger lattice mismatch, which will increase the probability of tunneling through the entire barrier. In addition, the quantum transmission coefficient ($T(\eta)$) of the electrons through the approximately triangular Schottky barrier without defects is given by[18]

$$T(\eta) = \exp\left(-\frac{4}{3}\frac{\sqrt{2m^*}}{\hbar}\omega\sqrt{\eta}\right), \tag{9}$$

where m^* is the electronic effective mass and $m^* = 0.22m_0$, m_0 is the free-electron mass, ω is the width of the tunneling barrier, and η is the energy offset from the conduction band at the metal/conductor interface as defined in Ref. [18]. According to Eq. (9), the quantum transmission coefficient $T(\eta)$ increases with the reduction of width of the tunneling barrier or the increase of the electric field of the barrier layer. Thus, the extremely thin barrier layer (3 nm) of AlN/GaN heterostructure induces a larger quantum transmission coefficient than does the barrier layer of AlGaN/GaN heterostructure. The current flow due to tunneling of electrons from the metal into the semiconductor without defects is given by

$$I_{m-s} = \frac{A^*ST}{k}\int_0^{qV_b} F_m T(\eta)(1-F_s)\,d\eta, \tag{10}$$

where A^* is the effective Richardson constant, S the Schottky contact area, F_m the Fermi–Dirac distribution function in the metal, F_s the Fermi–Dirac distribution function in the semiconductor, and V_b the bending of the conduction band. According to Eq. (10), the tunneling currents without defects under +0.1-V bias are calculated to be 1.24×10^{-7} A/cm^2 and 2.5×10^{-15} A/cm^2, which are much smaller than the values of $I_t(0)$. The tunneling current without defects decreases with forward bias increasing due to the reduction of the electric field of barrier layer. However, the defects existing in the barrier layer will reduce the effective width of the tunneling barrier, thereby increasing the tunneling current.

Table 2. Obtained values of tunneling saturation current, tunneling parameter, characteristic tunneling energy, series resistance, and DD for AlN/GaN and AlGaN/GaN Schottky diodes.

	$I_t(0)$/(A/cm^2)	E_0/eV	E_{00}/eV	R_S/Ω	D/cm^{-2}
AlN/GaN	3.77×10^{-6}	0.053	0.051	68.8	3.7×10^{9}
AlGaN/GaN	7.56×10^{-14}	0.032	0.027	66.6	5.5×10^{8}

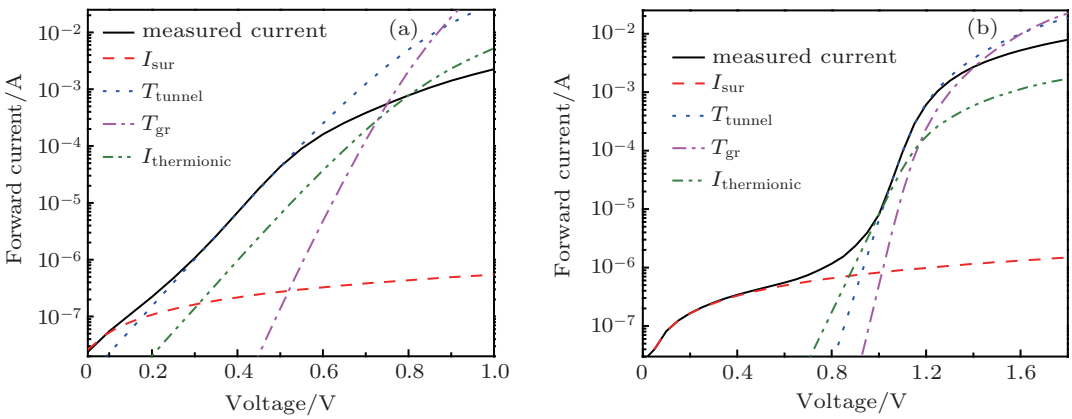


Fig. 4. (color online) The fittings of the TE, generation recombination, tunneling, and leakage current equation to the measured forward I–V data of the prepared AlN/GaN (a) and AlGaN/GaN (b) Schottky diodes.

Thus, the higher defect density and thinner barrier layer lead to the fact that the AlN/GaN Schottky diode suffers larger tunneling probability, larger leakage current, lower reverse breakdown voltage, and smaller turn-on voltage while maintaining a higher barrier height than AlGaN/GaN Schottky diode. The higher ideal factor (shown in Table 1) of the AlN/GaN Schottky diode further confirms the larger probability of tunneling through the entire barrier. So, optimizing the growth condition to reduce the defects and appropriately increasing the thickness of AlN barrier layer are crucial to reduce the leakage current and further improve the breakdown voltage of AlN/GaN device.

4. Conclusions

In this paper, Ni/Au Schottky contacts on AlN/GaN and AlGaN/GaN heterostructures are fabricated. The Schottky barrier height, the turn-on voltage, the ideal factor, and the reverse breakdown voltage of each sample are calculated and compared by self-consistently solving Schrödinger's and Poisson's equations from the measured *I*–*V* and *C*–*V* characteristics. It is found that the AlN/GaN Schottky diode has a larger Schottky barrier height but suffers larger leakage current and lower reverse breakdown voltage than the AlGaN/GaN Schottky diode. To explain the above phenomenon, the current mechanisms for AlN/GaN and AlGaN/GaN Schottky diodes are investigated by fitting the experimental *I*–*V* data to the analytical expressions given for the current-transport mechanisms including thermionic-emission, generation–recombination, tunneling, and surface leakage currents. Best fitting results are obtained for the tunneling current mechanism for both AlN/GaN and AlGaN/GaN Schottky diodes. However, the AlN/GaN heterostructure consumes more defects due to the larger lattice mismatch than AlGaN/GaN heterostructure. The higher defect density and thinner barrier layer in AlN/GaN Schottky diode well explain how the AlN/GaN Schottky diode suffers from larger leakage current and lower turn-on voltage while maintaining a higher barrier height than the AlGaN/GaN Schottky diode.

References

[1] Polyakov A Y, Smirnov N B, Govorkov A V, Markov A V, Yugova T G, Dabiran A M, Wowchak A M, Cui B, Osinsky A V, Chow P P, Pearton S J, Scherbatchev K D and Bublik V T 2008 *J. Appl. Phys.* **104** 053702

[2] Feng Q, Xing T, Wang Q, Feng Q, Li Q, Bi Z W, Zhang J C and Hao Y 2012 *Chin. Phys. B.* **21** 017304

[3] Ji D, Liu B, Lu Y W, Zou M and Fan B L 2012 *Chin. Phys. B* **21** 067201

[4] Shinohara K, Regan D, Corrion A, Brown D, Burnham S, Willadsen P J, Alvarado-Rodriguez I, Cunningham M, Butler C, Schmitz A, Kim S, Holden B, Chang D, Lee V, Ohoka A, Asbeck P M and Micovic M 2011 *IEDM Tech. Dig.* 19.1.1

[5] Cen L B, Shen B, Qin Z X and Zhang G Y 2009 *Chin. Phys. B* **18** 3905

[6] Shinohara K, Regan D, Corrion A, Brown D, Tang Y, Wong J, Candia G, Schmitz A, Fung H, Kim S and Micovic M 2012 *IEDM Tech. Dig.* 27.2.1

[7] Zhao Z J, Lin Z J, Corrigan T D, Wang Z, You Z D and Wang Z G 2007 *Appl. Phys. Lett.* **91** 173507

[8] Chen C H, Baier S M, Arch D K and Shur M S 1988 *IEEE Trans. Electron Dev.* **35** 570

[9] Lü Y J, Lin Z J, Meng L G, Yu Y X, Luan C B, Cao Z F, Chen H, Sun B Q and Wang Z G 2011 *Appl. Phys. Lett.* **99** 12354

[10] Cao Z F, Lin Z J, Lü Y J, Luan C B, Yu Y X, Chen H and Wang Z G 2012 *Chin. Phys. B* **21** 017103

[11] Lü Y J, Lin Z J, Zhang Y, Meng L G, Cao Z F, Luan C B, Chen H and Wang Z G 2011 *Chin. Phys. B* **20** 047105

[12] Arslan E, Altındal Ş, Özçelik S and Ozbay E 2009 *J. Appl. Phys.* **105** 023705

[13] Sze S M 1981 *Physics of Semiconductor Devices* (New York: Wiley)

[14] Yu A Y C and Snow E H 1968 *J. Appl. Phys.* **39** 3008

[15] Donoval D, Barus M and Zdimal M 1991 *Solid-State Electron.* **34** 1365

[16] Kotani J, Tajima M, Kasai S and Hashizume T 2007 *Appl. Phys. Lett.* **91** 093501

[17] Cheung S K and Cheung N W 1986 *Appl. Phys. Lett.* **49** 85

[18] Miller E J, Dang X Z and Yu E T 2000 *J. Appl. Phys.* **88** 5951